

Swiss Soft Days

13th Edition

Zurich, 14.02.2014



How/when to get there:

Welcome to the 13th Edition of the Swiss Soft Days!

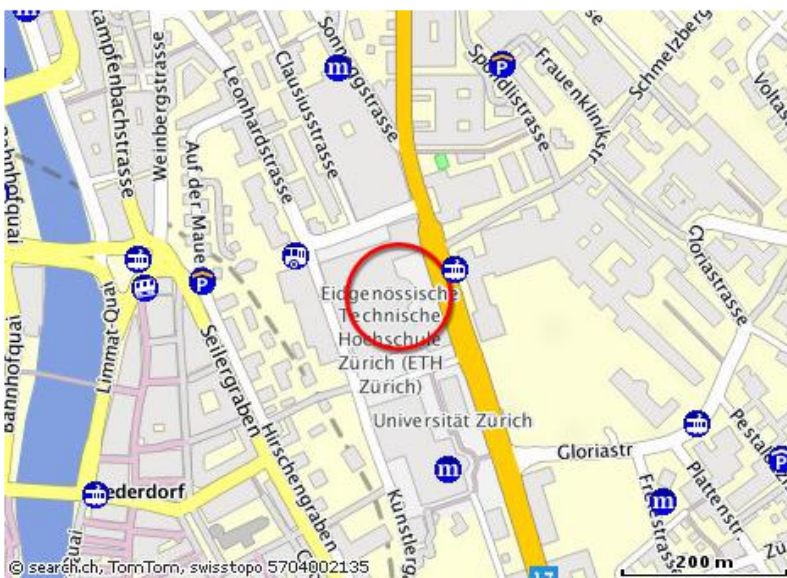
The conference venue is in the main building of ETH (HG Room E1.1) located in Rämistrasse 101

Address

ETH Zurich
Zentrum Campus

Rämistrasse 101
8092 Zurich
Switzerland

+41 44 632 11 11 →
+41 44 632 10 10 →



Please consider: The ETH Zurich uses for its location search maps from map.search.ch. In case a location is not registered, you can use the ETH Zurich pdf overview.

Travelling by public transport

Zurich Central Station

From the "Bahnhofstrasse/HB" stop

- Tram no. 6 ↓ (towards the Zoo) as far as the "ETH/Universitätsspital" stop
- Journey time: approx. 6 minutes

From the "Bahnhofplatz/HB" stop

- Tram no. 10 ↓ (towards the Airport or Oerlikon station) as far as the "ETH/Universitätsspital" stop
- Journey time: approx. 8 minutes

or

- Tram Nr. 3 ↓ (towards Klusplatz) as far as the "Central" stop (1 stop), from "Central" by Polybahn (departs every three minutes) to the Polyterrasse
- Journey time: approx. 8 minutes

Directions on how to reach the ETH main building can be found at the bottom of the map on the left. The venue can also be reached on foot within 10 to 15 minutes.

The conference room is located on the ground floor (E level) of the building and there will be signs directing to it.

The scientific program (see next page) will start at 10:30am. Registration and a welcome coffee will be available from 10am.

The program features two keynote speakers (Prof. Roberto Piazza, Milan Polytechnic and Prof. Chiara Daraio, ETH Zurich) and 9 short talks of 15 minutes each including questions. Time for additional discussions will be available during the breaks and the poster session.

The poster session will take place between 12:00 and 14:00, together with lunch, in the foyer in front of the lecture room. Poster boards and pins will be provided.

If you have any questions do not hesitate to contact us at lucio.isa@mat.ethz.ch

Have a happy meeting!

The local organizers

Emanuela Del Gado
Madhavi Krishnan
Peter Fischer
Lucio Isa

Scientific Program

10:00-10:30	Welcome Coffee/Registration	
10:30-11:15	Roberto Piazza	"Settled and unsettled issues in particle settling"
	Session 1: <u>Colloids</u> (Chair: Peter Fischer)	
11:15-11:30	Jader Colombo	"Stress Localization, Stiffening and Yielding in a Model Colloidal Gel"
11:30-11:45	Ahmet Demirörs	"Colloidal assembly directed by virtual magnetic mould"
11:45-12:00	Leonard Sagis	"Fibril-reinforced microcapsules produced by layer-by-layer assembly"
12:00-14:00	Lunch + Posters	
14:00-14:45	Chiara Daraio	"Exploiting nonlinearities in the design of new materials"
	Session 2: <u>Materials</u> (Chair: Emanuela Del Gado)	
14:45-15:00	Edmondo Benetti	"The Mediating Role of Polymer Brush Coatings on Scaffolds For Tissue Regeneration: From Poly(ethylene glycol) to Poly(oxazoline) Smart Grafts"
15:00-15:15	Duccio Malinverni	"Polymer Simulations in Slab Confined Geometry"
15:15-15:30	Isabelle Martiel	"A Reverse Micellar Mesophase of Face-Centered Cubic Fm3m Symmetry in Phosphatidylcholine/Water/Organic Solvent Ternary Systems"
15:30-16:00	Coffee Break	
	Session 3: <u>Microfluidics & Wetting</u> (Chair: Madhavi Krishnan)	
16:00-16:15	Marco Ramaioli	"Wetting of soluble coatings and its relevance to the dissolution of dehydrated beverage powders"
16:15-16:30	Claire Stanley	"Investigation of bacterial-fungal interactions using microfluidic platforms"
16:30-16:45	Daniele Vigolo	"Bubbles dancing in a vortex"
16:45-17:00	Tom Robinson	"Observations of lipid re-organisation in giant vesicles using microfluidics"
17:00-17:05	Closing remarks	

Keynote Speakers

Settled and unsettled issues in particle settling

Roberto Piazza

Department of Chemistry, Material Science, and Chemical Engineering “Giulio Natta”

Politecnico di Milano, via Ponzio 34/3, 20133 Milano, Italy

Colloid sedimentation has played a seminal role in the development of statistical physics thanks to the celebrated experiments by Perrin, which provided a concrete demonstration of molecular reality and gave strong support to Einstein's theory of Brownian motion. The aim of this talk, which mostly focuses on settling at low Peclet number where Brownian fluctuations are dominant, is to show that a lot more can be learnt both from the sedimentation equilibrium and from the particle settling dynamics of a wide class of systems, ranging from simple colloids to active particles and biological fluids, from foams to depletion gels. At the same time, the occurrence of unexpected and surprising effects brings about challenging questions in statistical and fluid mechanics that make sedimentation an exciting field of research.

Exploiting nonlinearities in the design of new materials

Chiara Daraio

*Department of Mechanical and Process Engineering, ETH Zürich
Tannenstrasse 3
Zürich, Switzerland*

Mechanics plays a central role in the design of new materials, providing the fundamental rules and guidelines for predicting the response of engineered systems. The starting points of our research are well understood nonlinear local phenomena, such as elastic Hertzian contact interactions between particles, or the deformation of micro- and nano-structures.

Exploiting these local phenomena, we develop new materials with novel global mechanical properties. By designing the structural geometry, we construct materials that can redirect mechanical waves, can absorb vibrations and impacts, or have very low thermal expansion coefficients

Oral Presentations

Stress Localization, Stiffening and Yielding in a Model Colloidal Gel

Jader Colombo and Emanuela Del Gado

ETH Zürich, Zürich, Switzerland.

We have investigated the mechanical response of a model colloidal gel under shear, with a new numerical procedure that allows us to follow deformations at relatively low shear rates. Moreover, differently from most existing numerical studies, we do not impose an artificial gel structure nor specific microscopic processes: the gel network and its mechanical response are the result of the interplay between the same effective interactions that stabilize the gel structure at rest and the imposed shear deformation. The effective interactions include a bending rigidity for the colloidal bonds and lead to the formation of a soft solid at relatively low solid volume fractions in a colloidal suspension, consistent with experimental observation. The load curve of the gel displays, after an initial linear elastic response, a significant stiffening and a final yielding (Fig. 1). By means of a space-resolved analysis of stresses and deformations in the gel network, we show that the strain hardening corresponds first to a progressive alignment of stresses and stretching of parts of the structure (chains or less connected parts of the gel network) along the direction of maximum extension under shear, and eventually to the shear deformations pulling on the over-stretched chains. We also find that the strain hardening of the gel is accompanied by an increasing stress localization, with the highest stress magnitude concentrating in few parts of the structure, where eventually breaking occurs (Fig.2).

Once yielding sets in, we observe the arising of shear induced density fluctuations in the gel that seems to coarsen into colloid-rich and colloid-poor domains. This phenomenon is apparently coupled to the onset of significant strain inhomogeneities in the material, which can be related to a shear banding, very similar to what observed in recent experiments. We have been able to elucidate here that the strain-induced reorganization of the gel and the shear banding are accompanied by an excess of crosslinks that are formed preferentially in the denser regions and therefore increase only the local stiffness of those domains, but not the overall capacity of the yielded gel to support higher stresses. The shear induced density fluctuations, the shear banding and the final level of stress attained in the gel upon yielding are strongly affected by the shear rate. Higher shear rates do not allow for rearrangements of the gel that can accommodate local changes in density, as signaled by a decreasing amount of non-affine displacements: this limits density fluctuations and the shear induced bond formation, resulting in higher stresses attained upon yielding.

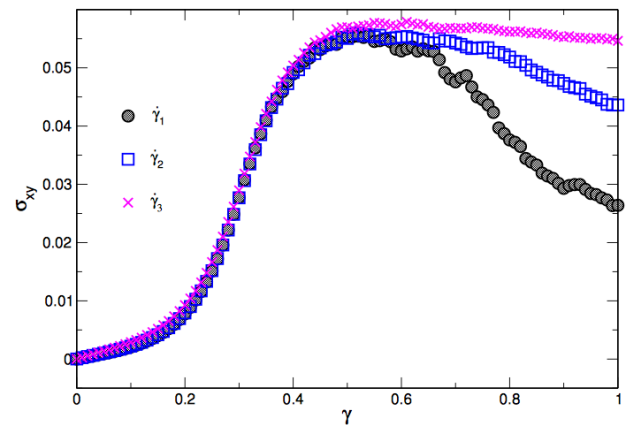


Fig. 1: Average shear stress plotted as a function of the shear strain, obtained in the model gel at different deformation rates.

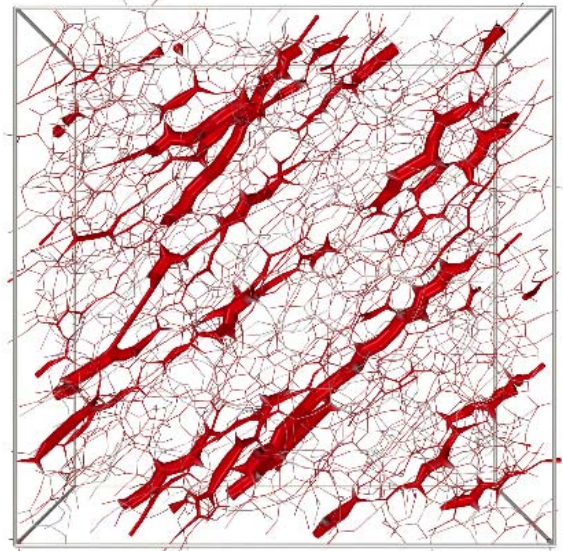


Fig.2: A snapshot of the gel network under shear: the thicker strands are the ones where the tensile stress intensity is larger than 60% of the maximum tensile stress.

Colloidal assembly directed by virtual magnetic mould

A.F.Demirörs^{1,2} P.P. Pillai¹ B. Kowalczyk¹ & B.A. Grzybowski¹

¹Northwestern University, Evanston, Illinois, USA. ²ETH Zürich, Zürich, Switzerland.

INTRODUCTION: Interest in assemblies of colloidal particles has long been motivated by their applications in photonics, electronics, sensors and microlenses. Existing assembly schemes can position colloids of one type relatively flexibly into a range of desired structures, but it remains challenging to produce multicomponent lattices, clusters with precisely controlled symmetries and three-dimensional assemblies. A few schemes can efficiently produce complex colloidal structures, but they require system-specific procedures.

RESULTS: Here,¹ we show that magnetic field microgradients established in a paramagnetic fluid can serve as virtual moulds' to act as templates for the assembly of large number of both non-magnetic and magnetic colloidal particles with micrometre precision and typical yields of 80 to 90 percent. We illustrate the versatility of this approach by producing single-component and multicomponent colloidal arrays, complex three-dimensional structures and a variety of colloidal molecules from polymeric particles, silica particles and live bacteria and by showing that all of these structures can be made permanent. In addition, although our magnetic moulds currently resemble optical traps in that they are limited to the manipulation of micrometre-sized objects, they are massively parallel and can manipulate non-magnetic and magnetic objects simultaneously in two and three dimensions.

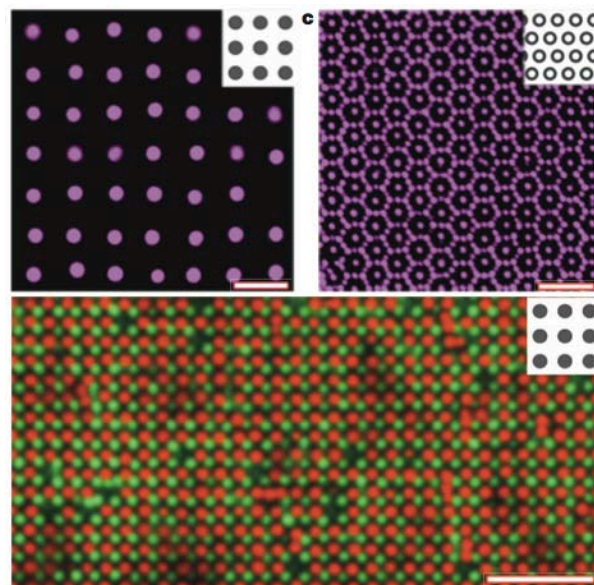


Fig. 1: Single-component (above) and multicomponent (below) colloidal arrays.

REFERENCES:

¹ A.F. Demirörs, P.P. Pillai, B. Kowalczyk & B.A. Grzybowski, *Nature*, 503, 99–103, 2013

ACKNOWLEDGEMENTS: This work was supported by the Non-equilibrium Energy Research Center, which is an Energy Frontier Research Center funded by the US Department of Energy, Office of Science, Office of Basic Energy Sciences under award number DE-SC0000989.

FIBRIL-REINFORCED MICROCAPSULES PRODUCED BY LAYER-BY-LAYER ASSEMBLY

L. M.C. Sagis^{1,2}, N.-P. Humblet-Hua¹,

¹ Wageningen University, Food Physics Group, Bornse Weiland 9. 6708WG Wageningen, The Netherlands. ²ETH Zurich, Dept. of Materials, Polymer Physics, Vladimir-Prelog-Weg 1-5/10, 8093 Zurich, Switzerland.

INTRODUCTION: Microencapsulation of functional ingredients is finding increasing application in food products, to improve or enhance nutritional value, or for preservation purposes. Food products cover a wide pH, temperature, and compositional range, and simple and flexible methods are needed to produce capsules for specific applications. Self-assembly of different layers of encapsulating materials on spherical emulsion droplets, driven by electrostatic interactions, can produce micron-sized capsules with well-defined barrier properties. The mechanical strength and permeability of the capsules can be controlled by varying the number of layers or by changing the characteristics of the encapsulation materials.

METHODS: We have produced capsules at acidic (pH 3.5) to slightly alkaline conditions (pH 8), using layer-by-layer adsorption, with either ovalbumin-pectin or lysozyme-pectin complexes for the flexible layers, and either long semi-flexible lysozyme fibrils (2-5 μm), short rod-like lysozyme fibrils (500-800 nm), or short flexible ovalbumin fibrils (200-300 nm), for the reinforcing layers (Fig. 1) [1]. We have compared mechanical strength of the capsules by studying their resistance against heat induced expansion.

RESULTS: We have found that for capsules with 5 or fewer layers, shells reinforced with flexible ovalbumin fibrils have higher mechanical stability than shells stabilized with long semi-flexible or rod-like lysozyme fibrils (Fig. 2) [1]. At higher number of layers, the lysozyme fibrils produce stronger shells than ovalbumin fibrils. Apparently, when longer stiffer fibrils are used, the mechanical strength of the capsules increase, but the shells are also more brittle [1].

DISCUSSION & CONCLUSIONS: We have shown that the mechanical stability of fibril reinforced multilayer microcapsules can be controlled by changing the length and flexibility of the reinforcing fibrils. Since food products are often processed at high deformation rates, flexible fibrils, may be a preferred reinforcing material over long rigid fibrils.

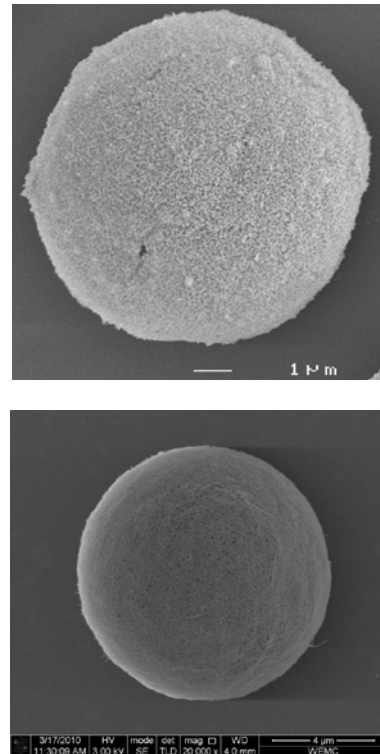


Fig. 1: Multilayer capsules reinforced with ovalbumin (top), or lysozyme fibrils (bottom).

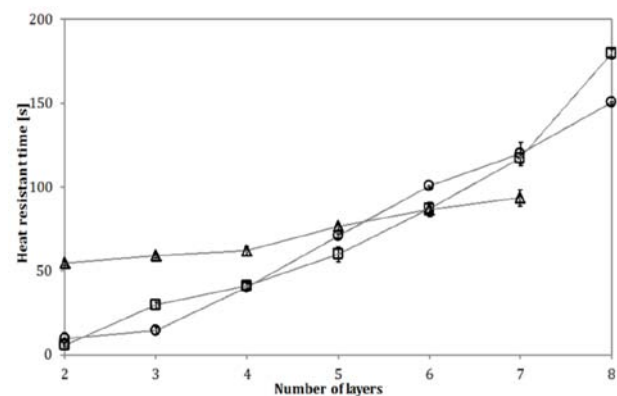


Fig. 2: Heat resistance time of microcapsules, exposed to a fixed temperature of 90°, reinforced with flexible ovalbumin fibrils (triangles) or stiff lysozyme fibrils (squares and spheres).

REFERENCES: ¹ K.N.P Humblet-Hua, E. van der Linden, L.M.C. Sagis; 2012; *J. Agric. Food Chem.*; 60: 9502 – 9511.

The Mediating Role of Polymer Brush Coatings on Scaffolds For Tissue Regeneration: From Poly(ethylene glycol) to Poly(oxazoline) Smart Grafts

Edmondo M. Benetti

Laboratory for Surface Science and Technology (LSST), Department of Materials, ETH Zürich, Wolfgang-Pauli-Strasse 10, 8093 Zürich, Switzerland

and

Materials Science and Technology of Polymers (MTP), Mesa+ Institute for Nanotechnology, University of Twente, P.O. Box 217, 7500AE Enschede, The Netherlands

Cells-biomaterials interactions have been increasingly studied in the last decade aiming to shed light on the mechanisms which govern cellular attachment and proliferation towards the generation of tissues. Growing efforts thus have been dedicated in replicating the characteristics of natural tissue by applying synthetic extra-cellular matrix (ECM) environments, paying particular attention to intimate structure, bulk physical properties and cytocompatibility. Both morphological and chemical structuring of surfaces were demonstrated to influence the behavior of adhering cells, with differences depending on cell type. Similar ECM manipulations were demonstrated to trigger a cascade of biomolecular events which eventually contribute in determining their fate.^{1,2} In this respect particular interest was devoted to stem cells and, specifically to human mesenchymal stem cells (hMSCs) as starting platforms for possible new tissue regeneration strategies.^{3,4}

Despite the widespread use of polymer brushes as surface modifiers for biomaterials, their specific functions as ECM-cells contact chemical and morphological mediators have not been conclusively studied, yet. Hence, we particularly focused on the specific response of hMSCs on polymeric scaffolds presenting functional brush coatings acting as “first contact layers”. We concentrated on poly(ethylene glycol) (PEG) and poly(methyl oxazoline) (PMOXA)-based grafts presenting functional moieties for anchoring cell adhesive biomolecules (fibronectin/collagen).

These polymeric surface modifiers have been applied on scaffolds by both “grafting-from” and “grafting-to” techniques. In the first case precisely tunable coating thicknesses have been obtained, in the second approach molecularly engineered polymer adsorbates formed highly functional adlayers.

The influence of composition, graft length (coating thickness) and graft density on the behavior of adhering stem cells were studied, for both these systems, establishing a relationship between the physical and chemical characteristics of the brush film and the response of hMSCs.

This research emphasized the role of ultra-thin brush films as ECM-cell mediating layers, umpiring and determining cells-scaffold interactions. Due to their intrinsic properties of robustness, high density and tunable configuration, polymer brushes were thus demonstrated as effective components in the designing of next-generation artificial ECM for stem cells

REFERENCES:

- 1) W. P. Daley, S. B. Peters, M. Larsen, *Journal of Cell Science* 2008, 121, 255.
- 2) F. Guilak, D. M. Cohen, B. T. Estes, J. M. Gimble, W. Liedtke, C. S. Chen, *Cell Stem Cell* 2009, 5, 17.
- 3) G. Chamberlain, J. Fox, B. Ashton, J. Middleton, *Stem Cells* 2007, 25, 2739.
- 4) P. Bianco, P. G. Robey, P. J. Simmons, *Cell Stem Cell* 2008, 2, 313.

Polymer Simulations in Slab Confined Geometry

[Duccio Malinverni](#)¹, [Paolo De Los Rios](#)¹,

¹ EPF Lausanne, Lausanne, Switzerland.

INTRODUCTION: Polymers in confined geometries are of growing interest in the fields of biophysics, physical chemistry, as well as in theoretical physics. Classical algorithms for sampling of long linear chain conformations in the canonical ensemble [2,3] break down in the limit of high-confined geometries, due to their prohibitively large rejection rates caused by the confinement [4]. A zero-rejection rate algorithm, with respect to confinement is presented. The main gain is a great decrease in correlation times of the Markov chain, which allow an efficient sampling of long chains in high confinement regime. Results of slab confinement effect on scaling regimes are presented and compared to analytical predictions. We observe quantitative agreement with theoretical predictions in the long-chain limit. Transient scaling regimes are observed and discussed.

METHODS: We proposed to study the equilibrium distribution properties of a single-polymer chain in slab-confinement. The polymer is modeled as a linear chain of cylindrical monomers, subject to bending stiffness and self-avoidance. The geometrical dimensions of the chains are tuned to reproduce experimental conditions of $(l_p \approx 50nm, \varnothing \approx 2nm)$ lambda-DNA. The slab confinement is modeled as a hard potential. The proposed sampling method is based on a Markov Chain Monte Carlo sampling scheme. Trial moves are decomposed in 2D pivot moves, taking advantage of the plane-symmetry of the slab (fig. 1). Vertical moves are composed of plane-perpendicular kink moves. Kink moves are constructed so to automatically generate configurations lying in between the two slab plates. This introduces a generation bias, which has to be corrected by suitably modifying the acceptance probability of the moves.



Fig. 1: The slab confinement. Polymer chains formed of cylindrical monomers are trapped between two parallel plates.

The overall procedure is analogous to Configurational Bias Monte Carlo (CBMC)

methods, where in our method the geometrical confinement plays the role of the self-avoiding chain in the CBMC.

RESULTS: Scaling results show agreement with analytical predictions in the asymptotical limit. The predicted scaling exponent in the infinite-chain limit follows the predicted 2D behavior (fig.2). In the central scaling region, between the linear and 2D regime, the Gaussian regime with exponent 0.5 is only qualitatively observed. Fitting the Gaussian and asymptotical regime with a bi-power law allows to extract the Gaussian to self-avoiding transition point. This fit allows to confirm a prediction of linear growth of the transition points with the slab width, based on Flory like arguments.

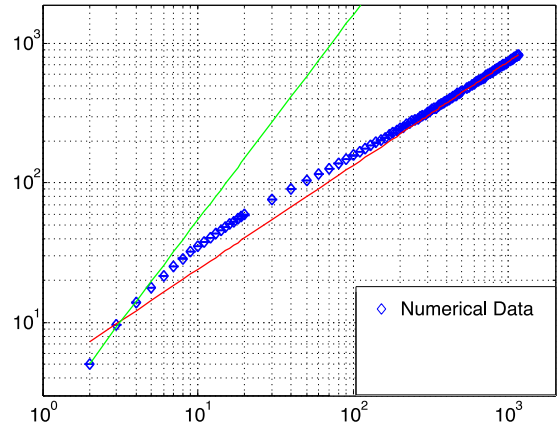


Fig. 2: Transient scaling regime. Asymptotically, the scaling follows the 2D prediction. The analytically predicted Gaussian regime can only be partially observed.

REFERENCES:

- [1] Hsu H-P., Grassberger P., J. Stat. Phys 2011, 144
- [2] Kennedy T., J. Stat. Phys 2002, 106
- [3] Madras N. , Sokal A.d., J. Stat. Phys 1987, 50
- [4] Micheletti C., et al., Phys. Reports 2011, 504
- [5] Reisner W., Pedersen J., Austin H, Rep. Progress in Phys. 2012, 75

A Reverse Micellar Mesophase of Face-Centered Cubic $Fm\bar{3}m$ Symmetry in Phosphatidylcholine/Water/Organic Solvent Ternary Systems

I.Martiel¹, L.Sagalowicz², R.Mezzenga¹

¹ Food and Soft Materials Science, Institute of Food, Nutrition & Health, ETH Zurich, Zurich, Switzerland. ² Nestlé Research Center, Vers-Chez-Les-Blanc, CH-1000 Lausanne 26, Switzerland.

INTRODUCTION: Phosphatidylcholine (PC) forms only lamellar mesophases in water, but it can be driven to self-assemble spontaneously into nonlamellar lyotropic liquid crystalline (LLC) mesophases by the addition of a third apolar component (oil) [2].

We report the formation of a *reverse* micellar cubic mesophase of symmetry $Fm\bar{3}m$ (Q^{225}) in ternary mixtures of soy bean PC, water, and an organic solvent, including cyclohexane, (R)-(+)-limonene, and isooctane, at room temperature [1]. The mesophase structure consists of a compact packing of remarkably large reverse micelles in a face-centered cubic (fcc) lattice, a type of micellar packing not yet reported for reverse micellar mesophases.

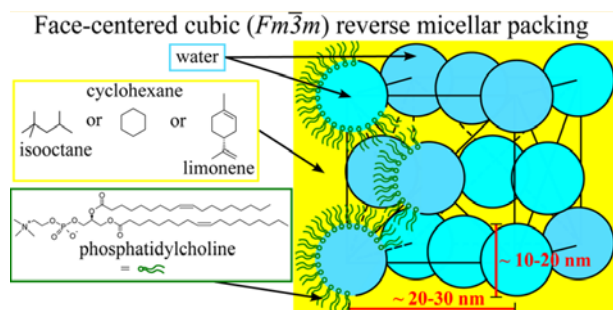


Fig. 1: Face-centered cubic (fcc) packing in the reverse $Fm\bar{3}m$ structure in PC/water/oil systems.

METHODS: Samples were equilibrated several weeks, and then characterized by Small Angle X-Ray Scattering (SAXS) and shear rheology. The $Fm\bar{3}m$ structure is compared with the non-compact $Fd\bar{3}m$ structure found in the PC/water/ α -tocopherol system. Form factor fitting in the pure L_2 phase and in the $Fm\bar{3}m$ - L_2 coexistence region yields quantitative estimations of the micellar low polydispersity and PC interface rigidity.

RESULTS: The mesophase spacegroup was identified based on spacing ratios and peak intensities. The variations of structural parameters point out to a classical hard-sphere phase diagram, showing an order-disorder transition $Fm\bar{3}m$ - L_2 with an extended coexistence region. Micellar polydispersities σ/R_c were systematically below 0.2, yielding interface rigidities $2k+k'$ of 1.6 to 2.0 $k_B T$.

DISCUSSION & CONCLUSIONS: The compact $Fm\bar{3}m$ structure results mainly from (1) the release of lipid tail frustration and (2) hard-sphere interactions between remarkably monodisperse micelles. The oil fills the large geometric voids of the fcc cell and modifies the interface bending properties by penetrating the PC tails.

Table 1: Indicative structural parameters for PC/water/limonene and PC/water/isooctane $Fm\bar{3}m$ phases.

	Limonene	Isooctane
Water capacity (wt. %)	33	50
Lattice parameter (nm)	19.9	31.5
Micelles radius (nm)	5.2	9.8
Plateau modulus (Pa)	$3.2 \cdot 10^4$	$1.5 \cdot 10^4$

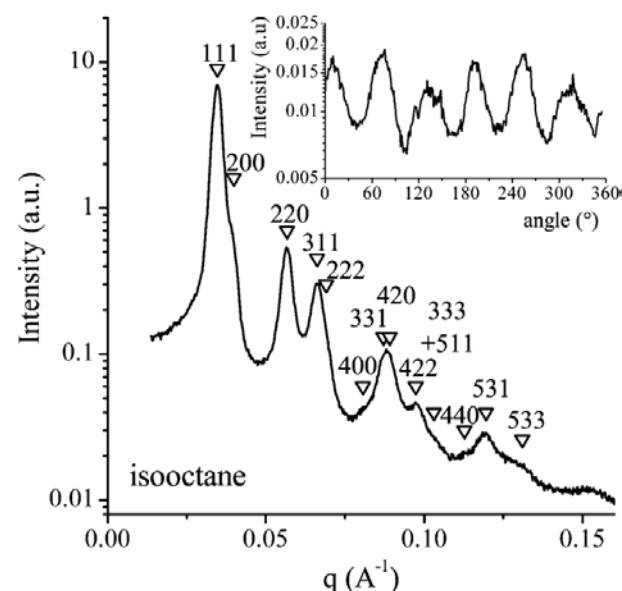


Fig. 2: SAXS pattern from a PC/water/isooctane $Fm\bar{3}m$ mesophase sample. Inset: azimuthal plot showing the 2D-hexagonal ordering in micelles layers.

REFERENCES: [1] I. Martiel, L. Sagalowicz, R. Mezzenga; **2013**; *Langmuir*; 29(51):15805-12. [2] R. Angelico, A. Ceglie, U. Olsson, G. Palazzo; **2000**; *Langmuir*; 20:2124-32.

ACKNOWLEDGEMENTS: This study was funded by NESTEC Ltd.

Wetting of soluble coatings and its relevance to the dissolution of dehydrated beverage powders

M. Ramaioli¹, J. Dupas², E. Verneuil³, L. Talini³, L. Forny¹, F. Lequeux³

¹ Nestlé Research Center - 1000 Lausanne 26, Switzerland.

² Nestlé PTC Orbe - 1350 Orbe, Switzerland.

³ PPMD, UMR7615 du CNRS, ESPCI, 75231 Paris, France.

When a powder is brought in contact with a solvent, a complex interplay of several phenomena conditions its dissolution. The reconstitution of a beverage by pouring a soluble powder onto water represents a typical example.

We study this complex problem by simplifying it into several model problems. In this study, we characterize the dynamic wetting of soluble coatings of maltodextrin [1, 2], an example of “reactive” wetting system.

The effect of contact line velocity, water content and coating thickness is discussed.

The role of water diffusion and the effect of the glass transition of the coating are elucidated.

These results allow deriving an upper bound for the capillary impregnation rate in soluble powders,

a phenomenon conditioning strongly their dissolution performance.

REFERENCES:

[1] J. Dupas, E. Verneuil, M. Ramaioli, L. Forny, L. Talini and F. Lequeux, Dynamic Wetting on a Thin Film of Soluble Polymer: Effects of Nonlinearities in the Sorption Isotherm, *Langmuir*, 29, 40, 2013.

[2] J. Dupas, E. Verneuil, L. Talini, F. Lequeux, M. Ramaioli, and L. Forny, Diffusion and evaporation control the spreading of volatile droplets onto soluble films, *Interfacial Phenomena and Heat Transfer*, Volume 1, Issue 3, 231-243, 2013.

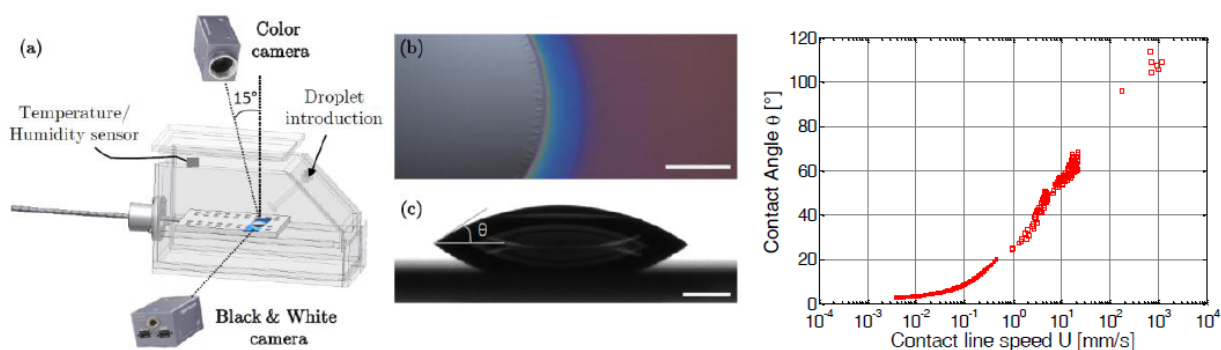


Figure 1. Experimental set-up and dynamic wetting angle of a water droplet on a maltodextrin thin coating.

Investigation of bacterial-fungal interactions using microfluidic platforms

Claire E. Stanley¹, Martina Stöckli², Dirk van Swaay¹, Pauli T. Kallio², Markus Künzler², Andrew J. deMello¹, Markus Aebi²

¹*Institute for Chemical and Bioengineering, Department of Chemistry and Applied Biosciences, ETH Zürich, Vladimir-Prelog-Weg 1, 8093 Zurich, Switzerland*

²*Institute of Microbiology, Department of Biology, Vladimir-Prelog-Weg 4, 8093 Zürich, Switzerland*

INTRODUCTION: A diversity of interactions exists between fungi and other microorganisms, which play central roles in certain human infections and the biological control of plant diseases.[1] However, studying the interplay between filamentous fungi and bacteria using high-resolution microscopies, and monitoring these interactions over a specific time period is technically challenging, since co-inoculation methods that are used at present have two major drawbacks: they either allow the study of interactions at the macroscale over time or on a cellular level at one specific time point. One major problem is due to the polarised growth of filamentous fungi. Hyphae form a three-dimensional interconnected network, which quickly leads to an overgrown system and therefore makes it challenging to follow a single hypha or hyphal compartment.

METHODS: Photolithography techniques [2] were used to produce microfluidic devices made from poly(dimethylsiloxane) (PDMS). Using these microfluidic platforms, individual hyphae of a filamentous fungus can grow into medium-filled microchannels from an agar plug that is placed next to a lateral opening. The height of the microchannels restricts the hyphae to a two-dimensional network (Fig. 1).

RESULTS: We have developed two microfluidic platforms that overcome the aforementioned problems, namely, the bacterial-fungal interaction (BFI) device and the fluid exchange device (Fig. 1). These devices were then used to study the interaction of *Coprinopsis cinerea* with two *Bacillus subtilis* strains (168 and NCIB 3610). In the BFI device, motile bacteria can be introduced into the microchannels through a separate inlet and are able to move freely within the channels. Morphological changes of hyphae, physical interactions and the distribution of bacteria in the channels can be observed using high-resolution microscopy at the single cell level over long lengths of time. The fluid exchange device allows rapid exchange of the fluid surrounding the hyphae. Using this platform, the response of

hyphae to different compounds can be studied readily. We observed a differential attachment of *B. subtilis* to *C. cinerea* hyphae. Further, it was found that *B. subtilis* NCIB 3610 produces a compound that leads to formation of blebs and emptying of hyphae.

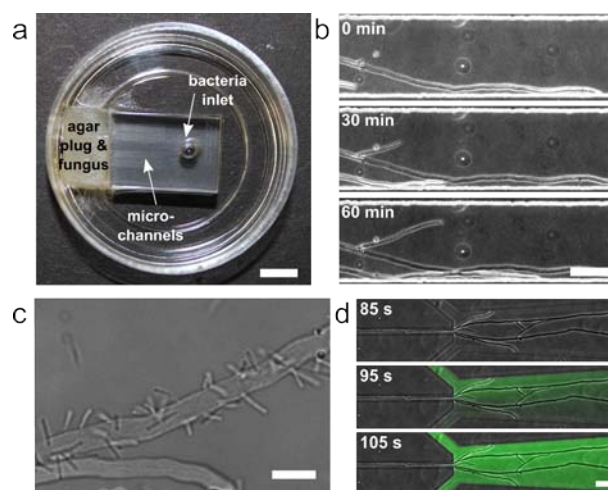


Fig. 1: (a) Bacterial-fungal interaction (BFI) device, (b) *C. cinerea* hyphae growing in a microchannel, (c) Interaction of *C. cinerea* with *B. subtilis*. (d) Fluid exchange device. Scale bars: 5 mm, 50 μ m, 10 μ m and 10 μ m respectively.

DISCUSSION & CONCLUSIONS: Our microfluidic approach offers a novel method to study cellular interactions that are imposed by nature. Specifically, they have been used to probe the interaction of *C. cinerea* with *B. subtilis*, providing – for the first time – new insights into this interaction at a cellular level and in real-time. The dynamics of the attachment and movement of the bacteria will be further studied in time and space using fluorescence microscopy.

REFERENCES: ¹ D. Hogan; 2002; *Science*; 296:2229-2232. ² D. Duffy; 1998; *Anal. Chem.*; 70:4974-4984.

ACKNOWLEDGEMENTS: J. Sabotic and C. Villalba for construction of plasmids, U. Sauer and R. Losick for providing *B. subtilis* strains, O. Dressler and A. Sheldon for custom software design and S. Stavrakis for microscopy advice.

Bubbles dancing in a vortex

Daniele Vigolo^{1,2}, Stefan Radl³, Howard A. Stone¹

¹ *Department of Mechanical and Aerospace Engineering, Princeton University, Princeton (NJ), U.S.A.*

² *Department of Chemistry and Applied Biosciences, ETH Zürich, Zürich, Switzerland.*

³ *Institute for Process and Particle Engineering, Graz University of Technology, Graz, Austria*

INTRODUCTION: A feature common to physiological as well as industrial and domestic flow systems is a bifurcation, or T-junction, that split the flow into two symmetric streams. We discovered that, unexpectedly, low-density particles or air bubbles dispersed in the solution can get trapped by the vortical structure that develops at the T-junction. Air bubbles then accumulate and increase in number, eventually changing size due to coalescence.

METHODS: We conduct experiments generating H_2 , O_2 or simply air bubbles in the range of Reynolds number, $Re = \rho v L / \mu$, where ρ is the fluid density, v the average flow velocity, L the lateral size of the channel and μ the viscosity, between 100 and 5,000, in a variety of T-junction with square section. We explore different lateral size devices ranging from 0.4 to 10 mm, and different air bubbles size. We also performed complete three-dimensional simulations of the pure fluid and the bubbly flow travelling through the T-junction.

RESULTS: Our experimental analyses revealed different behaviors depending on the Reynolds number. Starting from $Re = 100$, two symmetrical vortical structures develop at the T-junction. Air bubbles enter the vortices due to centrifugal forces and, surprisingly, for $Re > 220$, they get trapped, i.e., bubbles that enter the vortices are not leaving the bifurcation and accumulate (see Fig. 1A). For the same flow conditions our numerical simulations show the formation of a pressure gradient, similar to the vortex breakdown, at the core of the vortices directed towards the center of the T-junction. This pressure gradient is the responsible for the trapping phenomenon which is evident by the formation of four symmetric recirculation zones (see Fig. 1B). Bubbles eventually oscillate (i.e. “dance”) in the vortex when the flow becomes unsteady for $Re > 550$.

We then performed experiments on low-density rigid particles and on pulsed flow similar to physiological conditions, finding again the same trapping mechanism. We also experimentally observed a size dependent behavior of trapping which can be exploited to selectively trap, drag and separate different size of particles.

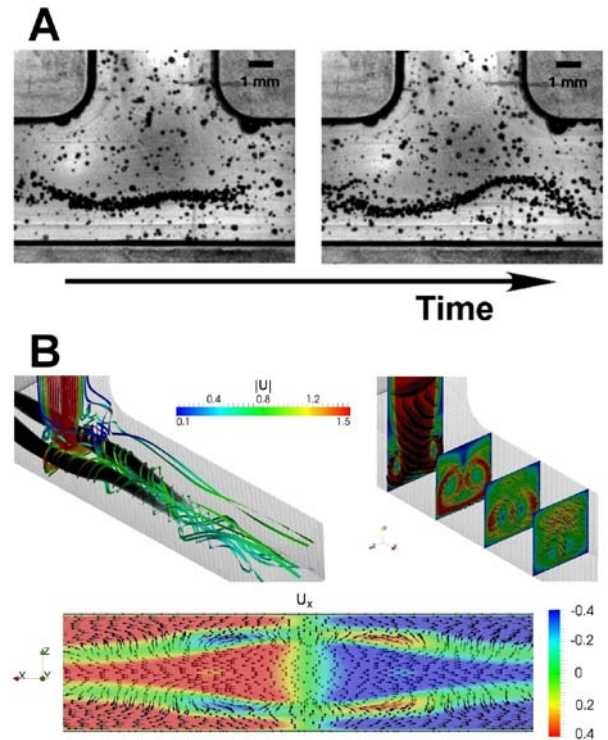


Fig. 1: Unexpected bubble trapping at a T-junction: (A) time-sequence images of an experiment showing bubble trapping for a device of lateral size $L = 4.8$ mm, and $Re = 980$; (B) 3D simulations showing the vortical structure and the four recirculating zones that develop at a T-junction for $Re = 500$.

DISCUSSION & CONCLUSIONS: The ubiquity of the geometry makes the trapping phenomenon that we unveiled extremely relevant for health, diagnostics and safety in industrial processes. In the presence of air bubbles or low-density material dispersed in the carrier fluid, it is important to control the geometry and the flow conditions to avoid or enhance this effect; for example, whenever the presence of a macroscopic air pocket is to be avoided, e.g., while designing a heat exchanger.

Observations of lipid re-organisation in giant vesicles using microfluidics

T.Robinson & P.S.Dittrich

Department of Chemistry and Applied Biosciences, ETH Zurich, Switzerland.

INTRODUCTION: As part of normal processes, cells experience various external forces such as mechanical pressure or fluidic shear stress and in turn, adapt and respond accordingly (1). Whilst the field of mechanobiology has been extensively studied, very little data exists on how lipid rafts within the cell membrane respond to these forces. Visualization of lipid rafts requires a model membrane such as giant unilamellar vesicles (GUVs) which are difficult to handle and confine. Here, we present how GUVs can be immobilized in a microfluidic device (2) and subjected to multiple forces, including mechanical loads. At the same time, the resulting spatial movement of phase-separated domains within the membrane can be observed by confocal microscopy.

METHODS: The device was fabricated using PDMS and consists of two layers. The bottom fluidic layer contains the GUVs while the top layer serves as a control layer. This control layer has two functions; to actuate (i) ring-shaped valves to partially isolate the vesicles from the fluid flow and (ii) to actuate circular micro-stamps for deforming the vesicles (Fig.1). These structures are aligned on top of a 60 microchamber array each with a trap able to capture a single GUV. Figure 2a shows a time-series of a trapped GUV being deformed as the mechanical load is increased. To analyse the lipids rafts, phase-separated GUVs are created by electroformation with a lipid mixture of sphingomyelin/DOPC/cholesterol. Fluorescent membrane dyes (NAP and DiI) were also incorporated, which partition into the liquid ordered (cholesterol-rich) and disordered phases, respectively. When flushed into the device, hydrodynamic trapping spatially confines more than 50 GUVs in a single device (2).

RESULTS: Without the addition of a mechanical load, the phase separation of the membrane is not expected to change in appearance due to being in a local energy minimum. By deforming the GUV, the appearance of the domains changes significantly, i.e. the lipids sort laterally in order to reduce this tension (Fig. 2). After release of the micro-stamp, the GUV goes back to its spherical shape but the domain patterns remain changed (Fig. 2b). In another example where a GUV exhibited two large domains (Fig. 2c), instead of observing an increase in the surface area, we measured a decrease due to the budding of domains.

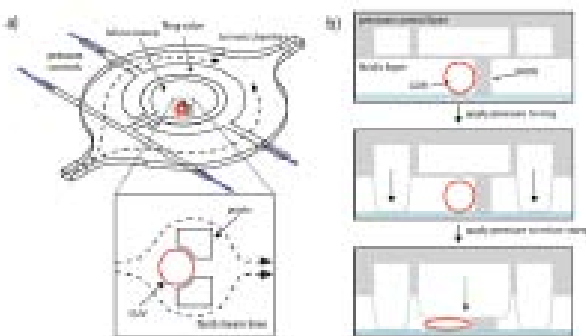


Figure 1: Schematic of the microfluidic device. a) Design of the microchambers with the control layer. Insert: once a GUV is trapped the fluid flow is diverted. b) Side view showing how the control layer, situated above the fluidic layer, can be actuated to lower the ring or micro-stamps.

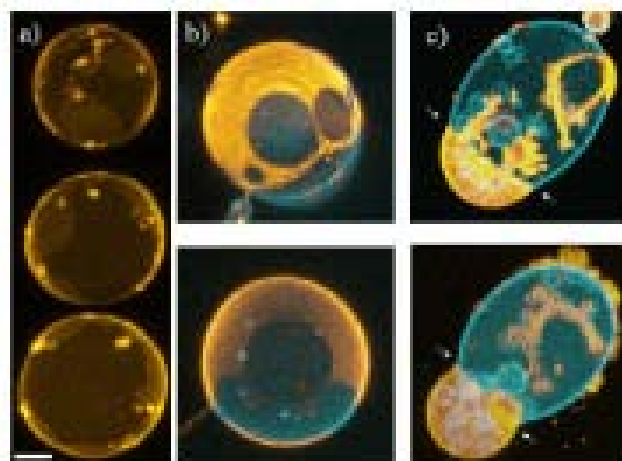


Figure 3. Deformed GUVs under a micro-stamp. a) Compression increases surface area. b) Domain patterns before and after the application of a mechanical load. c) Domains bulge out as a result of compression. Scale bar: 5 μm .

CONCLUSIONS: In conclusion, our method allows investigations on the molecular organization in membranes under mechanical loads.

REFERENCES:

1. O. P. Hamill and B. Martinac, *Physiological Reviews*, 81, 2 (2001).
2. T. Robinson, P. Kuhn, K. Eyer and P. S. Dittrich. *Biomicrofluidics*, 7, 4 (2013).

ACKNOWLEDGEMENTS: This work was funded by the European Research Council (ERC Starting Grant No. 203428, “ $\eta\mu$ LIPIDS”).

Posters

Entry flow of surfactant solutions through planar contractions

Lutz-Bueno, V.¹, Kohlbrecher, J.², Fischer, P.¹

¹ ETH Zurich, Zurich, Switzerland. ² PSI - Paul Scherer Institute, Villigen, Switzerland.

INTRODUCTION: The behavior of wormlike micelles flowing in a planar contraction-expansion flow-cell is investigated. Two samples differing by their concentration are examined using a combination of methods.

METHODS: The flow of two equimolar CTAB/NaSal micellar solutions belonging to dilute (2.5 mM) and semi-dilute (10 mM) regimes are investigated¹. The effects of extensional flow on the self-structuring of viscoelastic micelles are explored based on inertial effects, elasticity, vortex formation and flow-induced microstructural transitions. The use of a macroscopic 8:1:8 planar contraction-expansion flow-cell allows *in-situ* determination of micellar alignment by small angle neutron scattering (SANS) under influence of mixed flows. Other experimental techniques, including shear flow rheology, flow birefringence, particle image velocimetry are used.

RESULTS: The microstructure of wormlike micelles changes under shearing and extensional flows due to their self-assembling, growth and alignment, generating different bulk rheological behaviors. The SANS mapping of the flow cell is detailed in Reference 2. Based on it, a simple gray scale representation of the anisotropy factor (alignment of the micelles with the flow) with additional information of the flow direction was developed (Figure 1). The macroscopic alignment of the micelles was confirmed by flow birefringence.

DISCUSSION & CONCLUSIONS: The concentration of equimolar CTAB/NaSal solutions defines also their viscoelasticity. Solutions in the dilute regime form weak vortices, in which the micelles are influenced by shear and extensional flows. Semi-dilute surfactant solutions self-assemble into longer micelles, leading to higher viscoelasticity. The higher micellar alignment is along the centerline of the flow, where the extensional viscosity also influences. The entry flow is divided into two regions: the vortex region, where the micelles are influenced by the extensional flow, in a way that they are aligned and stretched forming a more viscous phase, and the recirculation region, where isotropic scattering is measured due to the formation of a stationary portion of flow with random micellar orientation. Longer vortices are generated by more viscoelastic fluids, as well as wider stationary flow regions under low volumetric flow rates.

REFERENCES: ¹ Lutz-Bueno, V.; Kohlbrecher, J. and Fischer, P. *Rheol Acta*, 2012, 52, 297–312. ² Lutz-Bueno, V.; Kohlbrecher, J. and Fischer, P. – submitted to *J. Non-Newtonian Fluid Mechanics*.

ACKNOWLEDGEMENTS: VLB acknowledges the financial support from ETH Zurich (Grant No. 0-20889-13) and PSI for the SANS measurement time.

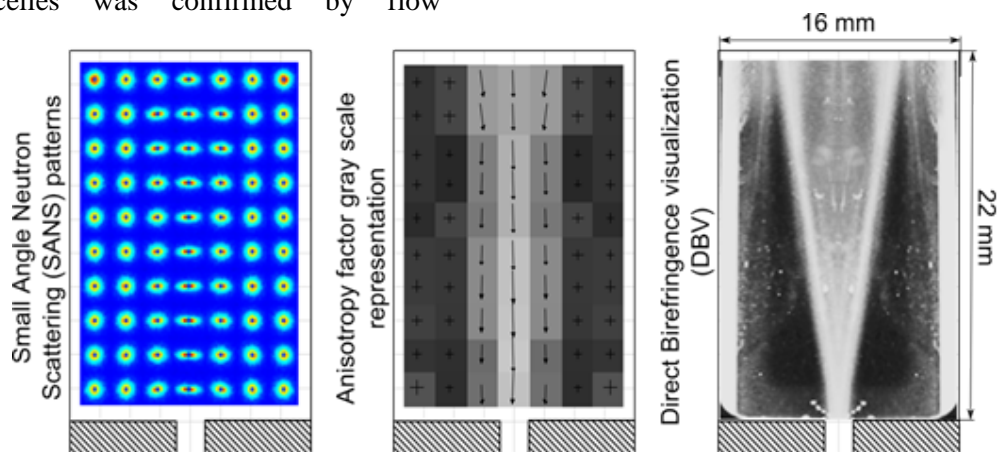


Fig. 1: Comparison between different methods of determining the alignment of wormlike micelles by the entry of a planar contraction.

Amphiphilic graft block copolymer PMOXA-graft(ss)-PCL synthesis and its potential application in drug targeting delivery

Dalin Wu, Adrian Najer, Cornelia. Palivan and Wolfgang Meier*

University of Basel, Basel, Switzerland.

INTRODUCTION: Amphiphilic block copolymers, especially with smart properties, due to can self-assemble into nanoparticles, are playing more and more important role in targeting delivery of chemical drug and gene drug.¹ Here, we are reporting a new type of graft amphiphilic block copolymer poly(2-methyl-2-oxazoline)-graft(ss)-poly(ϵ -caprolactone) (PMOXA-graft(ss)-PCL). The hydrophobic blocks connect with hydrophilic blocks through the redox responsive disulfide group, which can endow this polymer with redox property.

METHODS: We first synthesized the disulfanylpyridine modified PCL through the cationic ring opening polymerization of ϵ -caprolactone and α -benzyl carboxylate- ϵ -caprolactone. At the same time, the thiol ended PMOXA was synthesized through the ring opening polymerization of 2-methyl-2-oxazoline. Finally, couple the PCL and PMOXA through the thiol-disulfide exchange reaction with acetic acid as the catalyst. The chemical structures were characterized by ¹H NMR, GPC and FTIR. TEM and DLS were used to characterize the self-assembly results of these amphiphilic graft copolymers. The detailed research in controlling delivery of hydrophobic Dox, for example, was investigated by zeta-potential, fluorescence spectroscopy and LSM.

RESULTS: Three PMOXA-graft(ss)-PCL amphiphilic block copolymers were synthesized with different molecular weights, index of polydispersity and block ratio. All of these three block copolymers can self-assemble into nanoparticles with various size and polydispersity index (Fig. 1). In addition, the disulfide linker can be reduced by DTT or GSH in short time at room temperature (Fig. 1). The drug loading experiment demonstrated that hydrophobic Dox can be encapsulated into the nanoparticles which are formed by these three amphiphilic block copolymers (Table 1).

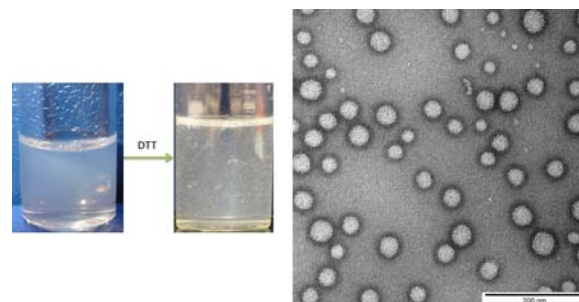


Fig. 1: DTT reduces the disulfide group(left); the typical TEM image of nanoparticles(right).

Table 1. The data of nanoparticles formed by hydrophobic Dox and PMOXA-graft(ss)-PCL.

entry	polymer (mg)	Dox (μ g)	z-average size (nm)	PDI	DLE(%)
1	1	50	41.7 \pm 11.7	0.17	37.5
	1	150	47.9 \pm 11.6	0.31	40.6
	1	250	53.5 \pm 12.9	0.33	40.9
2	1	50	33.4 \pm 9.8	0.25	34
	1	150	38.1 \pm 9.8	0.33	42.3
	1	250	44.9 \pm 8.6	0.49	42.8
3	1	50	35.3 \pm 6.3	0.3	34.7
	1	150	38.45 \pm 7.0	0.57	41.2
	1	250	41.5 \pm 6.2	0.71	33.3

DISCUSSION & CONCLUSIONS: The synthesized amphiphilic PMOXA-graft(ss)-PCL copolymer can encapsulate the hydrophobic drug Dox to form the nanoparticles with diameter from 30 nm to 50 nm depending on the amount of drug loaded into the nanoparticles. In addition, the nanoparticle size and PDI increased with the amount of fed drug. However, the drug loading efficiency (DLE) are around 40%, which seems have no relationship with the amphiphilic polymer and the amount of fed drug.

REFERENCES:1. Kelley, E. G. et al. Stimuli-responsive copolymer solution and surface assemblies for biomedical applications. *Chemical Society Reviews* **2013**.

ACKNOWLEDGEMENTS: This work was supported by the Swiss National Science Foundation, SNI and this is gratefully acknowledged. DW thanks China Scholarship Council for supporting the fee to study in abroad.

Impact of glass transition on crystallization process of charged colloids

F. Nazzani¹, M. Braibanti¹, V. Trappe¹

¹ University of Fribourg, Fribourg, Switzerland.

We explore the phase behavior of charged microgels at quasi-deionized conditions. At these conditions the microgels interact by long-range screened Coulomb interactions, which triggers the formation of crystalline phases over a large range of particle volume fractions. However, an increase in particle concentration also entails that the initial amorphous state, from which crystallization needs to arise, becomes increasingly frustrated. We investigate how both structural relaxation and elasticity of the amorphous phase impacts the crystal formation.

Our system is a suspension of charged PNiPAM microgels in water. The solvent is deionized using ion-exchange resins, so that the Coulomb repulsion among the particles is maximized. We use static and dynamic light scattering, to determine the structural and dynamical properties of the samples. All experiments are carried out in the q range accessible in a classical goniometer setup. Structure factors and fast relaxation processes are determined using a point detector scheme with a capability to resolve dynamics down to the nanosecond range. Slow relaxation processes are determined using a CCD, which also enables us to determine the instantaneous dynamics of the system by using the time resolved correlation scheme [1].

6 weeks after rejuvenation phase space can be divided in 2 regions: at low volume fractions the systems have reached equilibrium, exhibiting a transition between liquid and crystalline phases at $\phi=0.04$ (Fig.1-a).

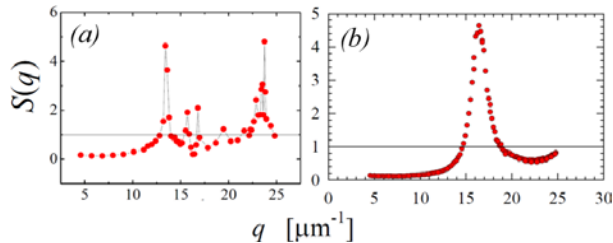


Fig. 1: Structure factors $S(q)$ observed at different volume fractions ϕ : a) BCC-FCC crystalline structures observed at $\phi=0.135$ vs. b) glassy structure at $\phi=0.260$.

At volume fractions higher than $\phi \approx 0.14$ the systems exhibit glassy features, showing that full equilibrium states cannot be reached. For $\phi < 0.26$

the samples exhibit partial crystalline order, while for $\phi > 0.26$ they remain fully glassy for extended periods of time (Fig.1-b).

The evolution of the instantaneous dynamics measured at peak q just after rejuvenation is smooth and exhibits only small fluctuations for $\phi < 0.14$. Instead at higher volume fraction ($\phi > 0.14$) giant fluctuations appear.

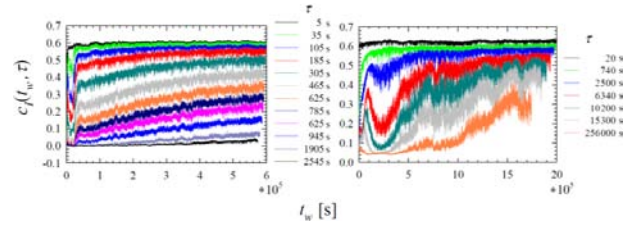


Fig. 1: Time-resolved correlation function for $\phi=0.135$ (left) and $\phi=0.260$ (right). Different lines show the degree of correlation measured for the lag time τ at the instant t_w .

The structural relaxation time τ exhibits an apparent divergence at $\phi \approx 0.14$, and beyond this volume fraction τ slowly increases with ϕ . At $\phi \approx 0.14$ we also observe that the α -decay of g_1 changes from a stretched exponential behaviour (for $\phi < 0.14$) to a compressed exponential behaviour (for $\phi > 0.14$) (Fig. 2).

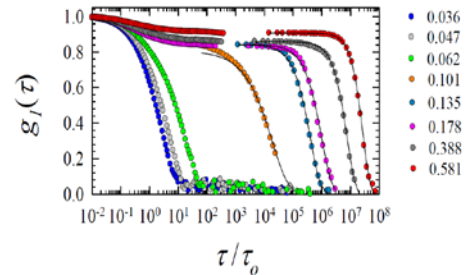


Fig. 2: Electric field autocorrelation function $g_1(\tau)$ measured at q peak position, for different volume fractions ϕ .

This implies a change in the origin of dynamics: from thermal-driven dynamics to a dynamics that is controlled by stress imbalances.

REFERENCES: ¹ L. Cipelletti et al. ; **2003**; *J. Phys.: Cond. Mat.*; 15:S257-S262.

We would like to thank to the University of Fribourg and the S.N.S.F. for funding

TEMPLATE-ASSISTED SYNTHESIS OF OPEN SILICA NANOSHELLS

Florian Guignard, Marco Lattuada

Adolphe Merkle Institute, Université de Fribourg, Route de l'Ancienne Papeterie CP 209, 1723 Marly 1, Switzerland

INTRODUCTION: In recent years many groups devoted their efforts in designing new types of anisotropic materials, which have a broader variety of properties than their isotropic counterparts. Janus nanoparticles are the prototype of anisotropic materials at the nanoscale. In this work we present a multistep synthesis to produce hollow Janus silica nanoshells having only one well-defined hole.

METHODS: The starting point is the synthesis of shape-anisotropic, asymmetrically-functionalized nanoparticles. We use a two-steps swelling procedure, where polystyrene seeds are first swollen and polymerized with a mixture of styrene and 3-trimethoxysilylpropyl methacrylate. Second, these coated seeds are once again swollen with styrene, giving birth to a dumbbell upon polymerization¹. These shape-anisotropic nanoparticles already have asymmetric surfaces, as only the first hemisphere contains silane moieties².

After washing, the dumbbells are reacted with a silane precursor, tetraethylorthosilicate (TEOS) which hydrolyses and condenses to form silica selectively on the hemisphere carrying silane group on the surface. We then remove the polymeric template either by calcination or by the dissolution of the polymer (which are not cross-linked) in tetrahydrofuran. The resulting nanostructure obtained is a Janus silica hollow shell bearing a hole, as a result of the TEOS not being condensed at the interface of the two polymeric hemispheres.

RESULTS: Silica capsules with a hole can be obtained in different size, depending on the seeds used in the very first step.

Depending on the how the polymeric template is removed, the inner wall of the shells is different. By calcination, the entire polymer is removed, leading to pure hydrophilic silica. In contrast, dissolution of the polymer in a suitable solvent like THF leaves a thin polymer layer on the interior of the shell, as some polystyrene chains are covalently bound to the silica via the 3-trimethoxysilylpropyl methacrylate moieties. We are now undergoing a variety of analysis to prove this difference.

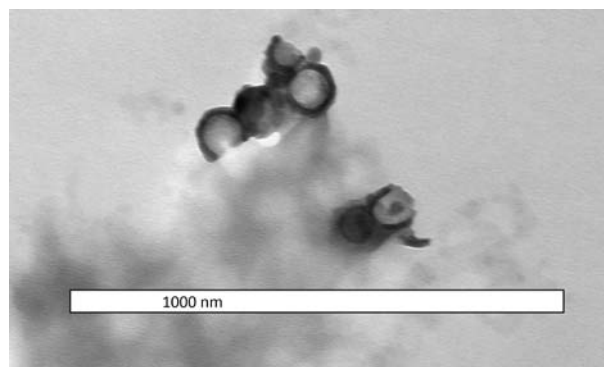


Fig. 1: Transmission electron microscope image of silica shells obtained by calcination of the polymer template.

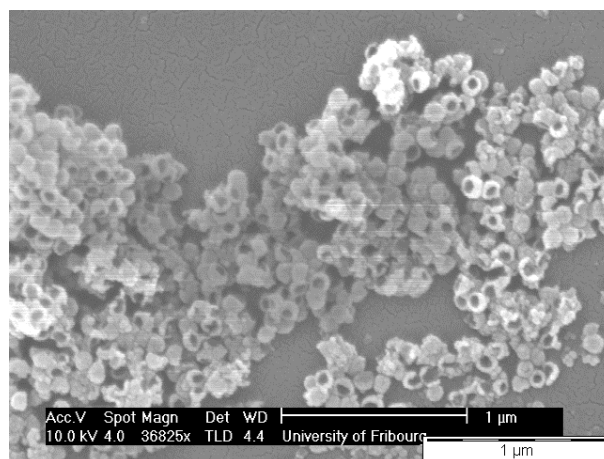


Fig. 2: Scanning electron microscope image of silica shells obtained by calcination of the polymer template.

DISCUSSION & CONCLUSIONS: A multistep synthetic procedure has been used to produce hollow silica shells with a hole. Many sizes can be targeted, by using seeds of different sizes. Depending on how the polymeric core is removed, nanoshells with their inner and outer surface bearing different functionalizations can be obtained.

REFERENCES:

- [1] Dufresne et.al, J. Am. Chem. Soc., 2010, 132, 5960-5961
- [2] F. Guignard, M. Lattuada, Chimia (Polymer and Colloid Highlights), **67**, 829 (2013).

WORM-LIKE micelles of polymerizable surfactant as a template for polymerization

[S.Rima](#), [M.Lattuada](#)

Adolph Merkle Institute, University of Fribourg, Fribourg, Switzerland.

The use of particles with anisotropic shape is of significant interest since it allows fabrication of structures with special symmetries and degree of packing, as well as with anisotropic properties. Rod-like polymer particles could have interesting properties and could find many practical applications; however, few methods for the production of such particles are available. In this work we introduced and investigate a simple method for synthesis of a new class of polymeric nanorods and nanofibrils based on emulsion polymerization using wormlike polymerizable micelles as template. Wormlike micelles, are elongated and semiflexible aggregates of surfactant molecules. The equilibrium and dynamics of the micellar structures, however, are determined by a delicate balance of intermolecular forces that can be easily disrupted. Addition of oils or polymers typically reduces the average micelle length and results in a dramatic decrease of the solution viscosity on the microstructure and loss of the highly elongated and entangled micelles. Solubilization and polymerization of styrene in different Cetyl trimethyl ammonium Tosylate (CTAT) wormlike solutions, at various: concentrations, temperatures and initiator systems, have been performed, and have been showed to preferentially form spherical particles. During the polymerization process, the viscosity is reduced by several orders of magnitude to a water-like value, and no viscoelasticity can be observed either visually or rheometrically.

These data suggest a transition from rodlike to spherical micellar aggregates. A polymerizable surfactant, cetyltrimethylammonium 4-vinylbenzoate (CTVB), containing a polymerizable counterion, has been prepared and investigated with the purpose of “locking in” the micellar structure over the oil polymerization so that the template is less sensitive to environmental changes. Elongated particles and long polymer fibrils have been formed depending on cross linker concentration used, partially preserving the structure of the parent micelle upon polymerization.

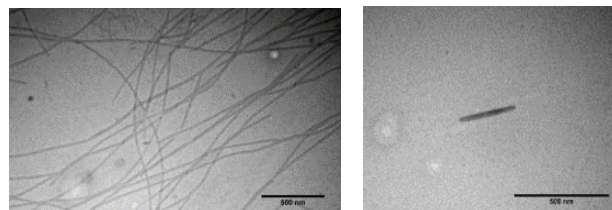


Figure 1 – TEM image of p(STY/DVB) fibrils and pSTY elongated nanoparticles.

Therefore, the presented approach represents a possible method for the production of anisotropic particles, with the purpose of studying their assembly for the preparation of nano- and microstructured materials.

Particle Ordering Using Inertial Microfluidics

Anandkumar S Rane, Xavier Casadevall i Solvas, Daniele Vigolo and Andrew deMello
 Insitute of Chemical and Bioengineering, ETH Zürich, Switzerland.

INTRODUCTION: Inertial effects in microfluidic channels are known to yield particle focusing at specific positions across the channel cross-section and a relatively uniform spacing (ordering) of particles along the channel length. Although the phenomenon of particle focusing has been characterized extensively [1], few studies have assessed the effect of experimental parameters on particle ordering; a key feature when designing devices for single cell encapsulation [2]. In this study, we have attempted to characterized particle ordering in inertial microfluidic devices by examining the influence of various experimental parameters like channel height and particle size on inter-particle spacing after particle focusing and ordering.

METHODS: Devices were based on both geometric and fluid dynamic parameters discussed in [1]. PDMS devices were fabricated using standard soft-lithographic techniques. Polystyrene beads (Sigma Aldrich) were used for all experiments. A representative device design is shown in Fig 1a, with the expected equilibrium positions along cross section of channel depending on its structure. A high-speed camera (MotionPro Y5, IDT, UK) was used to acquire bright-field movies of particle motion and in-house MATLAB codes were used to analyze particle ordering. Table 1 summarizes chip dimensions and other experimental parameters.

Table 1: Experimental Conditions

Experimental Parameter	Values
Channel Width (W: μm)	50
Channel Height (H: μm)	17-35
Particle diameter (d_p : μm)	8,10,12,15
Flowrates (Q: $\mu\text{L}/\text{min}$)	5-80

RESULTS: In our design we have constrained the height of Dean force-based channels with respect to particle diameter, and thus we expect particles to focus closer to the top and bottom channel walls (Fig 1a). Furthermore, we expect only one particle to occupy one of the two equilibrium positions at a given cross section of the device (Fig 1a). We observe that the particles are ordered in the direction of flow and large fraction of them tend to flow at a robust fixed interparticle distance (IPD) in the channel (Fig

1a). The particles order themselves in alternate configuration and have fixed IPD as compared to particles focused in same equilibrium position (Fig 1a). Fig 1b shows the variation of this fixed IPD with the height of the device for different particle diameters, under very good focusing conditions (high Reynold Number).

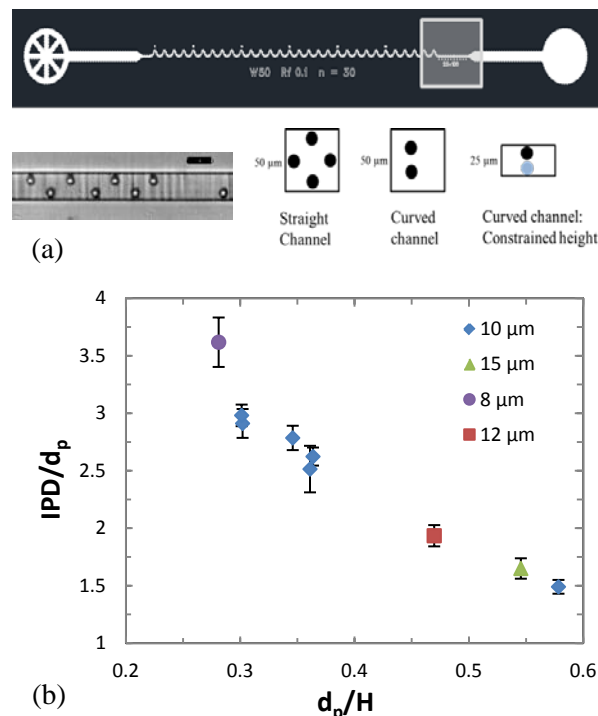


Figure 1: (a) Representative device design with expected equilibrium focusing positions (as viewed in cross-section) for straight and curved channels.

(b) Variation of observed interparticle distance to the height of the device.

DISCUSSION & CONCLUSIONS: The ratio of IPD to particle diameter decreases linearly with the ratio of particle diameter to the height of the device. We believe the observed trend in fixed inter-particle distance is a result of fluid-particle interaction and we are carrying out further investigations to better understand this phenomenon.

REFERENCES:

- ¹ D. Di Carlo; **2007**; *Proc. Natl Acad. Sci.*; **104**, 18892–7.
- ² J.F. Edd; **2008**; *Lab on a Chip*; **8**, 1262–1264.

Polymer Crystallization Assisted Thiol-ene Chemistry of a DNA Molecular Bottle Brush

Dawid Kedracki¹, Plinio Maroni¹, Helmut Schlaad² and Corinne Vebert-Nardin¹

¹ University of Geneva, Geneva, Switzerland², Max Planck Institute of Colloids and Interfaces, Research Campus Golm, Potsdam, Germany.

INTRODUCTION: Copolymer self-assembly is an elegant route to organize structures with sizes in the sub-micrometer range in solution and on surfaces. ¹Of high interest though is the propagation of the macromolecular properties to the ensemble inherent to this process. Copolymers organize into functional nanostructured materials with potential applications in various fields such as biomedicine, biomaterials engineering or catalysis. ² Having in mind future developments in biology and medicine, copolymers have thus been designed to assemble structures that might eventually enable the manipulation and comprehension of a biochemical mechanism to solve biological or medical issues in the future. Herein, we report on the polymer crystallization assisted thiol-ene synthesis of an amphiphilic comb/graft DNA copolymer composed of a hydrophobic poly(2-oxazoline) backbone and hydrophilic short single stranded nucleic acid grafts. In comparison to the straight solid phase supported synthesis of DNA block copolymers, photosynthesis enables achieving reaction efficiencies twice higher (above 60%) as evidenced by conventional chemical characterization.

METHODS: In order to characterize the macromolecular the morphology of the self-assembled structures as well as their potential for applications, the following techniques were used: dynamic light scattering (DLS) combined with static light scattering (SLS), electron microscopy (TEM, SEM) and confocal laser scanning microscopy (CLSM).

RESULTS The grafting of nucleic acid strands to poly (2-(3-butenyl)-2-oxazoline) (PBOX) could simply be obtained by exposing thio-terminated nucleotide sequence to PBOX microspheres (1:12 molar ratio) in degassed water to UV-visible light ($\lambda=305$ nm) over 24 h. Characterization evidence 67% reaction efficiency. Structure formation is induced by direct dissolution in aqueous solution under stirring. To achieve both sizing and refine the morphological determination, we combined multi-angle dynamic and static light scattering. DLS yields an apparent hydrodynamic radius R_H of 117 nm whereas SLS revealed a radius of gyration

R_G of 146 nm. The structures resulting from the self-assembly of the PBOX-g-DNA hybrids are therefore spheres constituted of about 20000 macromolecules. The functionality of the nucleic acid strands was assessed by hybridization assays. Around 30% of the nucleotide sequences engaged in the structure formation remain available for hybridization whereas 100% hybridization efficiency was monitored between the complementary sequences in solution.

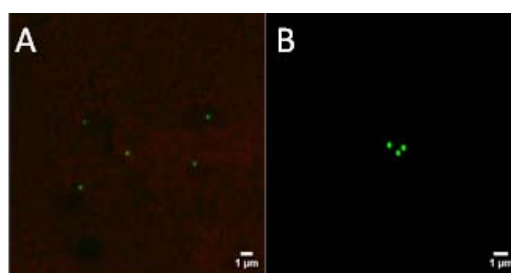


Fig. 1: CLSM evidences the speciation of complementary and non-complementary strands.

DISCUSSION & CONCLUSIONS: The experimental results demonstrate that the ability of the polymer to crystallize into microspheres could be used to carry out the synthesis of a PBOX-g-DNA molecular bottle brush and induce structure formation into sub-micrometer size structures that are stable against hydrogen bonding with nucleic acid strands present in the surrounding. These could therefore be used for the speciation of complementary and non-complementary strands both present in the surrounding. The functionality of the nucleic acid grafts paves the way to eventually utilize the self-assembled structures as three dimensional scaffolds to carry out organic reactions as well as for speciation of specific aptamer targets.

REFERENCES: ¹Mai Y., Eisenberg A., *Chemical Society reviews*, **2012**, *41*, 5969–85; ²Schacher F. H., Rugar P. a, Manners I., *Angewandte Chemie*, **2012**, *51*, 7898–921

ACKNOWLEDGEMENTS: The University of Geneva and the Swiss National Science Foundation for Research (PPOOP2-12838) are acknowledged for financial support.

Studying Complex Nanoparticle Self-Assembly at Liquid Interfaces Using Pendant Drop Tensiometry, Micro-rheology and Fluorescence Correlation Spectroscopy

[Adrienne Nelson](#), Dapeng Wang, Kaloian Koynov, Nicholas D. Spencer, Lucio Isa

Laboratory for Surface Science and Technology, Department of Materials, ETH Zürich, Switzerland

Max Planck Institute for Polymer Research, Mainz, Germany

Trapping at the interface, combined with lateral mobility and the presence of specific interactions, makes self-assembly of colloidal particles at liquid-liquid interfaces (SALI) a process with huge potential for the creation of controlled structures, including novel ultrathin membranes and capsules.

It has recently been demonstrated in our group that superparamagnetic iron oxide nanoparticles (NPs) stabilized by low molecular weight poly(ethylene glycol) (PEG) shells [1,2], can indeed be self-assembled into saturated monolayers at the water/*n*-decane interface [3,4]. Understanding the basics of SALI is a keystone in turning these NP assemblies into composite membranes suitable for applications. In particular, measuring the viscoelastic properties of the interfacial assemblies *in situ* and on the micro-scale is of paramount importance [5].

Characterisation of particles using pendant drop tensiometry (PDT) and dynamic light scattering has been completed at different concentrations in order to compare the effects of different PEG shells on the behaviour of the particles. Measurements have been carried out on particles stabilised with different molecular weight and architecture (linear versus dendritic) PEG. Particles with longer linear PEG chains show the highest surface activity and the fastest kinetics of adsorption.

To further investigate the behaviour of the nanoparticles at the decane-water interface, two techniques have been used to characterise the mechanical properties of the interface via the tracking of probe particles with very different sizes. Micron-sized tracer particles observed with fluorescence optical microscopy still show

diffusive behavior at the interface upon adsorption of the NPs, with a moderate effect on the diffusion coefficient depending on the different architectures of the NP shells. Fluorescence correlation spectroscopy (FCS), using quantum dots as tracers [6], was used to investigate the mechanical behavior of the interfacial monolayers on the same length scale of the nanoparticles. Surprisingly, also the nanoscale tracers showed purely diffusive behavior at the interface, with a progressive slowing down ascribed to NP adsorption. It was thus possible to follow the build-up of the NP monolayer at the interface with time (NP adsorption), as previously observed with the PDT measurements, and to obtain master curves for the diffusion coefficient as a function of a concentration-dependent effective time.

REFERENCES:

- [1] E. Amstad, T. Gillich, I. Bilecka, M. Textor, E. Reimhult; **2009**, *Nano Lett* 9:4042–4048.
- [2] T. Gillich, C. Acikgo, L. Isa, A. D. Schlueter, N. D. Spencer, M. Textor; **2013**, *ACS Nano* 7:316–329.
- [3] L. Isa, E. Amstad, M. Textor, E. Reimhult; **2010**, *Chimia* 64:145–149.
- [4] L. Isa, E. Amstad, K. Schwenke, E. Del Gado, P. Ilg, M. Kroege, E. Reimhult; **2011**, *Soft Matter* 7:7663–7675.
- [5] F. Ortega, H. Ritacco, R. G. Rubio, **2010**, *Current Opinion in Colloid & Interface Science* 15:237–245.
- [6] D. Wang, S. Yordanov, H. M. Paroor, A. Mukhopadhyay, C. Y. Li, H. Butt, and K. Koynov, **2011**, *Small* 7:3502–3507.

In-situ measurements of the wetting properties of individual micro and nanoparticles at liquid-liquid interfaces

Lucio Isa

Laboratory for Interfaces, Soft matter and Assembly, Department of Materials, ETH Zürich, Switzerland

New materials obtained by the self-assembly of micro- and nanoparticles (MPs and NPs) at liquid interfaces hold the potential to impact many technological applications, including functional membranes and delivery vehicles. Despite impressive developments in the synthesis of complex MPs and NPs, the quest for a general way to control the properties of the final material starting from the properties of the building blocks still faces outstanding open challenges. True progress is often hindered by the lack of control and *in situ* characterization of the basic particle properties and of the way in which they interact.

I will describe a recently developed methodology, based on freeze-fracture and cryo-SEM, which allows us for the first time to measure *in situ* at liquid interfaces the three-dimensional location, and thus the contact angle, of individual particles as small as 10 nm in diameter [1,2]. I will present its application to several systems of

practical interest including deformable hydrogel particles used as novel emulsion stabilizers [3], surfactant adsorption for double emulsion inversion [4] and highly hydrophobic nanoparticles used in microfluidic emulsification [5]. I will also highlight the potential of the method in elucidating fundamental aspects of single-particle wetting, including controlled shape and surface chemistry anisotropy.

REFERENCES:

1. L Isa, F Lucas, R Wepf and E Reimhult, *Nature Communications*, 2:438, 2011
2. L Isa, *CHIMIA*, 67 (4), pp. 231-235, 2013
3. K Geisel, L Isa and W Richtering, *Langmuir*, 28 (45), pp. 15770–15776, 2012
4. BP Binks, L Isa and AT Tyowua, *Langmuir*, 29 (16), pp. 4923–4927, 2013
5. J S Sander, L Isa, P Rühs, P Fischer, and A R Studart, *Soft Matter*, 8, pp. 11471-11477, 2012

Controlling local packing and growth in calcium–silicate–hydrate gels

K. Ioannidou¹, Roland J.-M. Pellenq² and Emanuela Del Gado¹

¹ *ETH Zurich, Department of Civil, Environmental and Geomatic Engineering*

² *MIT, Department of Civil and Environmental Engineering; CNRS and CINaM, Aix-Marseille University*

We investigate the development of gels under out-of-equilibrium conditions, such as calcium–silicate–hydrate (C–S–H) gels that form during cement hydration and are the major factor responsible for cement mechanical strength. We propose a new model and numerical approach to follow the gel formation upon precipitation and aggregation of nano-scale colloidal hydrates, whose effective interactions are consistent with forces measured in experiments at fixed lime concentrations. We use Grand Canonical Monte Carlo to mimic precipitation events during Molecular Dynamics simulations, with their rate corresponding to the hydrate production rate set by the chemical environment. Our results display hydrate precipitation curves that indeed reproduce

the acceleration and deceleration regime typically observed in experiments and we are able to correctly capture the effect of lime concentration on the hydration kinetics and the gel morphology. Our analysis of the evolution of the gel morphology indicates that the acceleration is related to the formation of an optimal local crystalline packing that allows for large, elongated aggregates to grow and that is controlled by the underlying thermodynamics. The defects produced during precipitation favor branching and gelation that end up controlling the deceleration. The effects on the mechanical properties of C–S–H gels are also discussed.

Nesting of anomalies in supercooled silicon

Vishwas V Vasisht¹, John Mathew² and Srikanth Sastry³

¹*Institut f. Baustoffe (IfB), ETH, Zuerich, Switzerland*

²*Dept. of Condensed Matter Physics and Materials Science, Tata Institute of Fundamental Research, Mumbai, India.*

³*TIFR Centre for Interdisciplinary Sciences, Hyderabad, India.*

Anomalous behaviour in density, diffusivity and structural order is investigated for silicon modeled by the Stillinger-Weber potential by performing molecular dynamics simulations. As previously reported in the case of water [Errington and Debenedetti, *Nature*, 409, 318, 2001] and silica [Shell et al., *PRE*, 66, 011202, 2002], a cascading of thermodynamic, dynamic and structural anomalous regions is also observed in liquid silicon. The region of structural anomaly includes the region of diffusivity anomaly, which in turn encompasses the region of density anomaly (which is unlike water but similar to silica). In the region

of structural anomaly, a tight correlation between the translational and tetrahedrality order parameter is found, but the correlation is weaker when a local orientational order parameter (q_3) is used as a measure of tetrahedrality. Excess entropy and the pair correlation entropy is calculated and scaling relations, proposed by Rosenfeld and Dzugutov, associated with diffusion coefficient is verified. The correlation between the excess entropy and the regions of anomalies in the phase diagram of liquid silicon is examined.

Measuring the properties of single nanoscale objects in solution using an electrostatic fluidic trap

F.Ruggeri¹, M.Krishnan^{1,2}

Dept. of Chemistry¹ & Dept. of Physics²

University of Zürich, Zürich, Switzerland.

INTRODUCTION: Single nanoscale objects in solution can be trapped in three dimensions in a fluidic nanoslit. Tailoring the geometry of the walls of the slit gives rise to an electrostatic free energy landscape, where local potential wells passively confine single charged entities for long periods [1]. Relating the statistical properties of a trapped object's motion to a free energy calculation permits a direct measurement of its charge [2].

METHODS: We study Brownian motion of single nanoscale objects trapped in harmonic confining potentials. The statistical properties of the trapped object's motion in x , y and z reveal the stiffness of confinement, k and k_z in the radial and axial dimensions, which yields a measure of the object's charge [2]. Figure 1 presents scatter plots in x , y , z for a single 80 nm diameter negatively charged gold particle. The measured standard deviations in lateral displacement, s_r are directly related to the spring constants of confinement via $k = 2k_bT / s_r^2$. Comparing the measurement with a calculated spring constant yields a direct measurement of the charge of an individual particle (Fig. 2).

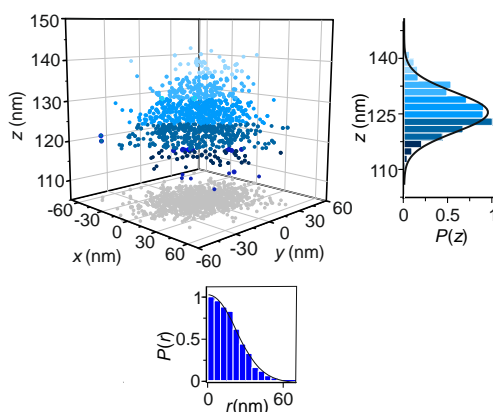


Fig. 1: Analysis of the three-dimensional motion of a single particle trapped in a harmonic potential well.

We obtain the spatial electrostatic potential distribution by solving the nonlinear Poisson Boltzmann equation for the full 3D system. The Gibb's free energy, F of the system is then calculated as a function of particle position (r, z) for a range of values of particle charge, q [3]. For

a nano-structure designed to give a harmonic trapping potential, the spatial free energy profile can be fit to a function $\Delta F = kr^2$

to yield the spring constant, k_{calc} . We find that k_{calc} is linear over a wide range of q (Fig. 2).

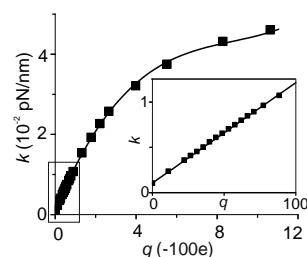


Fig. 2: The charge on an object can be read off directly from the calculated k vs q relation.

RESULTS AND DISCUSSION: Comparing the experimentally measured spring constant k with the theoretically expected k_{calc} directly reveals the charge on single particle (Fig. 3).

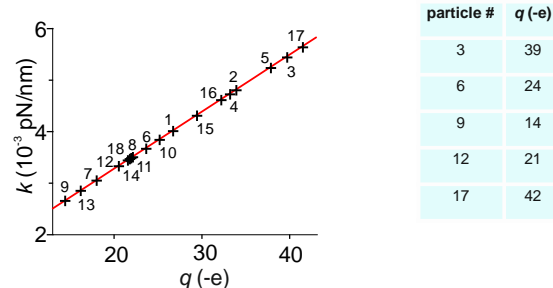


Fig. 3: Representative single particle charge measurements

We believe that passive trapping could be used to measure the charge of nano-objects, e.g. single proteins, ribosomes, and macromolecular complexes. Furthermore with this technique it could be possible to study two- and three-body interactions in a trap and measure in real time fluctuations in total charge of associating/dissociating complexes.

REFERENCES: ¹ Krishnan, Mojarad, Kukura & Sandoghdar, *Nature* 467 (2010) 692-695.

² Mojarad & Krishnan, *Nature Nanotechnology* 7 (2012) 448-452.

³ Krishnan, *J. Chem. Phys.* 138, 114906 (2013)

Short time measurement of interfacial tension in liquid/liquid systems

P. Fischer¹

¹ Institute of Food, Nutrition and Health, ETH Zürich, 8092 Zürich, Switzerland.

Dispersing of bubbles and droplets takes place in the millisecond range. New interface is generated and eventually stabilized by surfactants or other surface-active molecules. Adsorption starts as soon as the pure interface is accessible to the molecules. Common methods to measure the interfacial tension have a time lag of at least 0.01 s for liquid-liquid interfaces. Important information on the adsorption kinetics, which can be determine important properties such as emulsion and foam stability are therefore not accessible. The discussed approach measures the liquid-liquid transient interfacial tension by a combination of gravity and flow induced droplet detachment (Figure 1) summarized in a force balance [1, 2].

$$0 = \underbrace{3 \cdot \pi \cdot \eta_{cont} \cdot v_{cont} \cdot (d_{drop} - d_{cap})}_{\text{extended Stokes equation (drag force)}} - \underbrace{\pi \cdot \gamma \cdot d_{cap}}_{\text{interfacial tension force}} + \underbrace{\pi \cdot d_{drop}^3 \cdot g \cdot \frac{\Delta \rho}{6}}_{\text{gravitation and buoyancy}} + \underbrace{\pi \cdot \gamma \cdot \frac{d_{cap}^2}{d_{drop}}}_{\text{Laplace pressure force}} + \underbrace{4 \cdot \rho_{disp} \cdot \frac{Q_{disp}}{\pi \cdot d_{cap}^2}}_{\text{momentum transfer}}$$

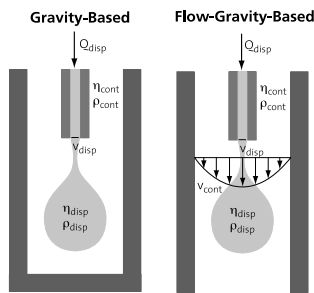


Fig. 1: Gravity and flow-gravity based approaches to measure the interfacial tension.

The short time adsorption kinetics of two surfactants, Lecithin and Imbentin, are studied in a water-in-oil system as shown in Figure 2. The drop diameters are plotted as a function of the velocity of the continuous phase which contains different emulsifier concentration. The drop diameter where all curves merge corresponds to a drop formation time of 5 ms. From this velocity of the continuous phase the Lecithin molecules have not sufficient time to adsorb at the interface because of the short drop formation times less than 5 ms. Consequently, the interface remains "clean" and the drop diameters conform to the drop diameters of the pure liquids. In contrast, Imbentin shows in all cases a reduction of the droplet size meaning that the surfactant molecule is able to reach and adsorb at the newly created interface at all drop formation times down to 4 ms.

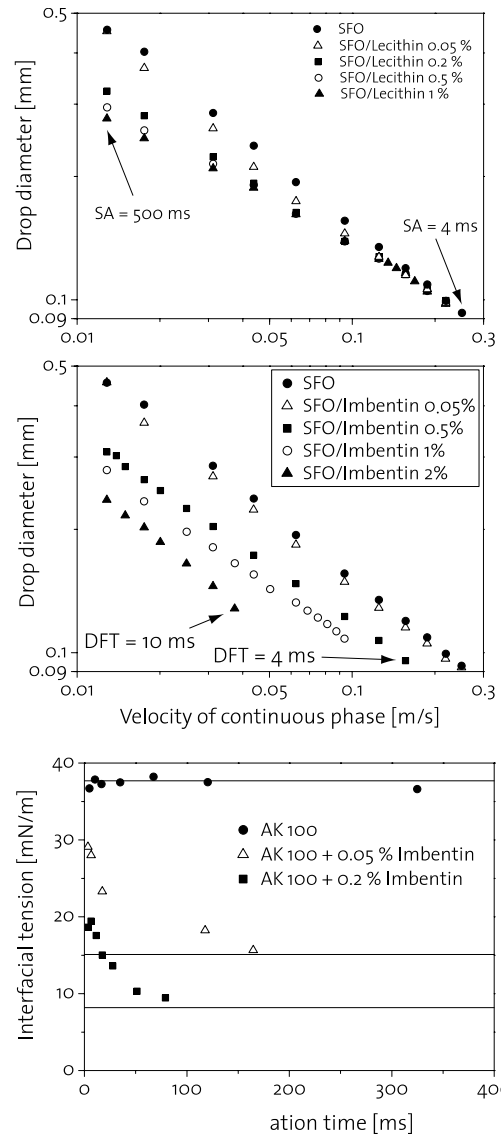


Fig. 2: Droplet diameter as a function of the velocity of the continuous phase for fluids with different concentrations of Lecithin and Imbentin (water/k-Carrageenan 0.38 wt.% in sunflower oil). Calculation of the transient interfacial tension according to Equation 1.

REFERENCES:

- [1] Cramer C, Fischer P, Windhab EJ: Drop Formation in a Co-Flowing Ambient Fluid, *Chemical Engineering Science* 59 (2004) 3045-3268
- [2] Cramer C, Studer S, Windhab EJ, Fischer P: Periodic dripping dynamics in a co-flowing liquid-liquid system, *Physics of Fluids* 24 (2012) 093101

Controlling Satiety by Tailored Interfaces

N. Scheuble¹, A. Steingötter², P. Fischer³

¹ *Institute of Food, Nutrition and Health, ETH Zürich, 8092 Zürich, Switzerland.* ² *Division of Gastroenterology and Hepatology, University Hospital Zurich, 8091 Zurich, Switzerland and* *Institute for Biomedical Engineering, ETH Zürich, 8092 Zürich, Switzerland.*

The use of oil-in-water emulsions as tailored fat delivery systems with defined breakdown pathways is a possible strategy to fight obesity [1]. Fat lead to overconsumption as it involves palatability, what determines dietary preferences [2]. Controversy, its sensory properties implement neuronal responses, which correlate with a short-term control of appetite and satiety [3]. After ingestion of dispersed fat, the rate and activation of lipolysis and associated satiating hormonal responses, is determined by the emulsion stabilization and the size of the fat droplets [4]. Therefore, by designing interfacial layers, lipase activity and lipid release, may be modified. Hence, we established a model system of a protein-biopolymer adsorption layer with composite material properties, making the interface stable during exposure to the gastric environment (temperature, pH, mechanical stress, enzymes, etc.). Such model layers will be scaled up to lipid emulsions. Their lipid release during digestion will be validated *in vivo* by Magnetic resonance imaging, and thus emulsions can be further optimized.

Interfacial shear rheological experiments of α -lactoglobulin have shown that the well deformable, viscoelastic layer softened at body temperature and during acidification. Besides, it degraded by the exposure to pepsin. The polysaccharide methylcellulose built a highly elastic, but brittle interfacial layer. It further gelled during temperature increase and remained stable during pH reduction and pepsin exposure. With the combination of both biopolymers, synergistic layer characteristics were concluded. A shear-stable,

viscoelastic layer was formed, which resisted during pH reduction and pepsin exposure. Moreover, the combination of neutron reflectivity, atomic force microscopy and surface pressure experiments showed coexistence and interactions of the two materials at the interface. The knowledge gained from this study lead to a new understanding in the research area of controlled lipid release and therefore helps for future food and drug formulations.

REFERENCES:

- [1] Norton I, Moore S, Fryer P: Understanding food structuring and breakdown: engineering approaches to obesity, *Obesity Reviews* 8 (2007) 83-88.
- [2] Gaillard D, Passilly-Degrace P, Besnard, P: Molecular Mechanisms of Fat Preference and Overeating, in *Addiction Reviews 2008 – Annals of the New York Academy of Science* 1141 (2008) 163-175.
- [3] Rolls E, Critchley HD, Browning AS, Hernadi I, Lenard L: Responses to the sensory properties of fat of neurons in the primate orbitofrontal cortex, *Journal of Neuroscience* 19 (1999) 1532-1540.
- [4] Golding M, Wooster T, Day L, Xu M, Lundin L, Keogh J, Clifton P: Impact of gastric structuring on the lipolysis of emulsified lipids, *Soft Matter* 7 (2011) 3513-3523

Interplay of drainage and coalescence in SDS-foams

D. Calzolari¹, D.Z. Gunes², A. Salonen³, F. Restagno³, E. Rio³, V. Trappe¹

¹*Physics Department, University of Fribourg, Ch. Du Musée 3, CH-1700 Fribourg, Switzerland*

²*Department of Food Science and Technology, Nestlé Research Center, Vers-chez-les-Blanc, Lausanne 26, CH-1000, Switzerland*

³*Laboratoire de Physique des Solides, UMR CNRS 8502, Université Paris-Sud, 91405 Orsay cedex, France*

We present ongoing investigations about the interplay of coalescence and drainage governing the instability of foams, using SDS-foams with a fixed initial liquid fraction of $\varepsilon_0=0.25$ and bubble size of $a_0=25\ \mu\text{m}$. The foams are produced by the turbulent mixing of nitrogen and SDS-water-glycerol solutions with a fixed viscosity of $\eta=45\ \text{mPa}\cdot\text{sec}$ that contain various amounts of NaCl. For these foams the coalescence rate can be directly observed at the top of the foam.

We find that liquid drainage and coalescence are directly correlated, both becoming faster with increasing NaCl content. The rather intuitive scenario that the screened electrostatic interactions determine the speed of film rupture and thus coalescence, which in turn determines the speed of the release of liquid, does not account for the observed behavior.[1,2] Instead, these preliminary results support the idea that the decrease in the surface elasticity with increasing NaCl content allows for a faster drainage, which in turn entails a faster coalescence.[3-5]

REFERENCES

- [1] L. Wang, R.-H. Yoon, *Int. J. Miner. Process.* **85** 101–110 (2008)
- [2] V. Carrier, A. Colin, *Langmuir* **19**, 4535-4538 (2003)
- [3] T. Tamura, Y. Kaneko, M. Nikaido, *J. Coll. Int. Sci.* **190** 61-70 (1997)
- [4] S. Sett, S. Sinha-Ray A.L. Yarin, *Langmuir* **29** 4934-4947 (2013)
- [5] L. Saulnier et al., *Soft Matter* DOI: 10.1039/C3SM52433G (2014)